

DOI:10.1002/ejic.201402735

Solution Speciation of the Dinuclear Zr^{IV}-Substituted Keggin Polyoxometalate [$\{\alpha\text{-PW}_{11}\text{O}_{39}\text{Zr}(\mu\text{-OH})(\text{H}_2\text{O})\}_2\}^{8-}$] and Its Reactivity towards DNA-Model Phosphodiester Hydrolysis

Thi Kim Nga Luong,^[a] Gregory Absillis,^[a] Pavletta Shestakova,^[a,b] and Tatjana N. Parac-Vogt*^[a]

Keywords: Polyoxometalates / Zirconium / Hydrolysis / Kinetics / NMR spectroscopy

The solution speciation of the Zr^{IV}-substituted Keggin polyoxometalate (Et₂NH₂)₈[$\{\alpha\text{-PW}_{11}\text{O}_{39}\text{Zr}(\mu\text{-OH})(\text{H}_2\text{O})\}_2\} \cdot 7\text{H}_2\text{O}$ (ZrK 2:2) was fully determined under different pD, temperature, and concentration conditions. Subsequently, phosphodiester bond hydrolysis of the DNA model substrate bis(4-nitrophenyl) phosphate (BNPP) promoted by ZrK 2:2 was studied in detail. In the presence of ZrK 2:2, phosphoester bond hydrolysis in BNPP proceeded with a rate constant of $k_{\text{obs}} = (4.75 \pm 0.25) \times 10^{-6} \text{ s}^{-1}$ at pD 6.4 and 60 °C, which represented a 320-fold rate enhancement relative to the spontaneous hydrolysis of BNPP. The pD dependence of k_{obs} exhibits a bell-shaped profile, with the fastest rate observed at pD

6.4. An activation energy (E_a) of 60.16 kJ mol⁻¹, enthalpy of activation (ΔH^\ddagger) of 57.44 kJ mol⁻¹, entropy of activation (ΔS^\ddagger) of -173.16 J mol⁻¹ K⁻¹, and Gibbs activation energy (ΔG^\ddagger) of 111.12 kJ mol⁻¹ at 37 °C were calculated. The influence of the concentration of ZrK 2:2 on the reaction rate constant was studied in the concentration range 0.5 to 6.0 mM. The results showed that ZrK 2:2 is able to hydrolyze an excess amount of BNPP, thus demonstrating that ZrK 2:2 acts as a catalyst for phospho(di)ester bond hydrolysis. In addition, the influence of ionic strength and the inhibitor diphenyl phosphate on BNPP hydrolysis were examined.

Introduction

Polyoxometalates (POMs) are a large class of inorganic oxoclusters that contain early-transition metals (V, Nb, Ta, Mo, and W) in their highest oxidation state.^[1] Their chemically robust nature and highly tunable chemical and physical properties (including acidity, thermal stability, redox potential, solubility, size, shape, and charge) have resulted in their broad application in material science,^[2] magnetism,^[3] and catalysis.^[4] In addition, several classes of POMs have been reported to have potent antitumor, antiviral and antibacterial properties, thereby resulting in a substantial interest in the potential medical application of POMs.^[5]

To gain insight into the biological activity of POMs, we have recently examined the reactivity of several POMs towards different biologically relevant molecules and their model systems. For example, it was shown that polyoxovanadates and -oxomolybdates are active towards phospho-

ester,^[6] carboxyester,^[7] and peptide-bond hydrolysis.^[8] Interestingly, the incorporation of different transition-metal ions with high Lewis acidity (Zr^{IV} and Ce^{IV}) into heteropolyoxometalates of the Keggin, Wells–Dawson, and Lindqvist type resulted in catalysts that also displayed hydrolytic activity towards phosphoester bonds,^[9] and amide bonds in peptides and proteins.^[10] In addition, Zr^{IV}-substituted POMs have been shown to be efficient Lewis acid catalysts in different organic transformations such as Mukaiyama aldol and Mannich-type reactions, H₂O₂ and sulfide oxidation reactions, and the cyclization of citronellal.^[11]

Phosphate esters play several important roles in biological systems including information storage (DNA/RNA), energy transduction (ATP), and cellular signaling (cAMP).^[12] The phosphodiester bonds in these molecules are extremely resistant towards hydrolysis primarily because of the repulsion between the negatively charged backbone and potential nucleophiles.^[13] At room temperature and in the absence of a catalyst, the half-life for phosphodiester bond hydrolysis has been estimated to be 130000 years for DNA at neutral pH, and four years for RNA at pH 6.0.^[14] This stability makes them excellent systems for information storage.^[15] However, despite the extreme stability of the phosphoester bond, its efficient cleavage is often a required procedure in biochemistry, and for this purpose efficient cleaving agents are needed.

[a] Laboratory of Bioinorganic Chemistry, Department of Chemistry, KU Leuven, Celestijnenlaan 200F, 3001 Leuven, Belgium
E-mail: Tatjana.Vogt@chem.kuleuven.be
www.chem.kuleuven.be/lbc/

[b] NMR Laboratory, Institute of Organic Chemistry with Centre of Phytochemistry, Bulgarian Academy of Sciences, Sofia, Bulgaria

Supporting information for this article is available on the WWW under <http://dx.doi.org/10.1002/ejic.201402735>.

In nature, phosphomono-, -di-, and -triesther bonds are often hydrolyzed by the cooperative action of two or more adjacent metal ions.^[16] These can be Mg^{II}, Zn^{II}, Mn^{II}, and/or Fe^{III}. For example, in alkaline phosphatase, a nonspecific phosphomonoesterase, the active site contains two Zn^{II} centers and one Mg^{II} ion. Both Zn^{II} ions are involved in (1) the binding and Lewis acid activation of the substrate, (2) the activation and delivery of the nucleophile, and (3) stabilization of the pentacoordinate transition state and leaving group. However, the active site of its low-pH analogue, purple acid phosphatase, is composed of two iron centers in the mammalian form, whereas kidney bean purple acid phosphatase is a Zn^{II}/Fe^{III} metalloenzyme, as is also the case for calcineurin, a serine/threonine phosphatase involved in T-cell activation.

Over the years, artificial organic monometallic and bimetallic model compounds that mimic bimetallic phosphatases and nucleases have been synthesized.^[17] They typically consist of Co^{III}, Cu^{II}, Zn^{II}, Ni^{II}, Fe^{III}, or Ce^{IV} and are being studied to unravel the mechanism of enzymatic action on the one hand, and to develop artificial catalysts for phosphoester bond hydrolysis for biochemical and industrial applications on the other. Recently, our group demonstrated the first example of phosphoesterase activity of a metal-substituted polyoxometalate complex.^[9] The Zr^{IV}-substituted Wells–Dawson POM K₁₅H[Zr(α₂-P₂W₁₇O₆₁)₂]-25H₂O has been shown to catalytically hydrolyze phosphoester bonds in 4-nitrophenyl phosphate (NPP) and bis(4-nitrophenyl) phosphate (BNPP), both of which are commonly used DNA substrates. Zr^{IV} is ideally suited as an active center in artificial hydrolytic metalloenzymes because of its high Lewis acidity that results from its +IV oxidation state, and its oxophilic properties, which are beneficial for coordinating and activating both the substrate and the nucleophile. In addition Zr^{IV} can adopt an eight-coordination state, which allows better interaction with the substrate than most of the other transition metals, which are typically six-coordinate.

Model compounds such as NPP, BNPP, and 2-hydroxypropyl 4-nitrophenyl phosphate (HPNP) are frequently used when assessing the reactivity of newly developed artificial phosphatases and nucleases. They offer the advantage of being composed of good leaving groups, thereby improving the reactivity of the model compound under study relative to the natural enzyme substrates. Despite the presence of these good leaving groups, BNPP is still extremely resistant to hydrolysis and is characterized by a half-life of about 75 years at pH 7.0 and 50 °C^[18] and 2000 years at pH 9.2 and 25 °C.^[19]

In this study, the phosphoesterase activity of the dinuclear Zr^{IV}-substituted Keggin-type POM (Et₂NH₂)₈{α-PW₁₁O₃₉Zr(μ-OH)(H₂O)}₂·7H₂O (ZrK 2:2) has been examined towards the phosphodiester DNA model compound BNPP. Owing to its bimetallic nature and the bridged character of both metal centers, which leaves free coordination sites for the binding and activation of the substrate and nucleophile, this POM represents a better mimic for the active site in natural phosphatases and nucleases rel-

ative to the Wells–Dawson-type K₁₅H[Zr(α₂-P₂W₁₇O₆₁)₂]-25H₂O POM. Moreover, we have previously shown that ZrK 2:2 effectively catalyzed amide-bond hydrolysis in different peptides and proteins, thus demonstrating its ability to act as an effective Lewis acid catalyst.^[10c,20] As the solution speciation of this POM is highly dependent on pH, temperature, and initial POM concentration, a detailed aqueous solution study has also been performed to optimize the reaction conditions.

Results and Discussion

Solution Speciation of ZrK 2:2

Depending on the synthesis conditions, Zr^{IV}-substituted Keggin POMs can be prepared in two forms: as a ZrK 2:2 POM,^[10c,21] which represents a dinuclear Zr^{IV} complex sandwiched between two monolacunary α-Keggin POMs (Figure 1, a), and as a ZrK 1:2 POM,^[22] which consists of a mononuclear Zr^{IV} ion sandwiched between two monolacunary α-Keggin POMs (Figure 1, b). Since the maximum coordination number of Zr^{IV} is eight,^[21] the free coordination sites available for substrate complexation to each Zr^{IV} ion are most likely 1 in the 2:2 structure and 0 in the 1:2 structure. Therefore the ZrK 2:2 POM is expected to have better catalytic activity than the ZrK 1:2 species.^[11b]

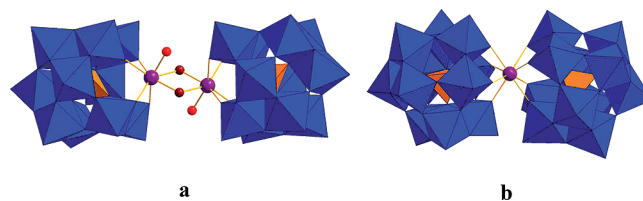


Figure 1. Structures of (a) ZrK 2:2 and (b) ZrK 1:2. The WO₆ groups are represented by blue octahedra, whereas the internal PO₄ groups are represented by orange tetrahedra. Zr^{IV} and H₂O molecules are represented by violet and red balls, respectively.

The stability of ZrK 2:2 and the equilibria that occur in aqueous solution between the different Zr^{IV}-substituted Keggin-type POMs were examined in detail with the aim of determining the optimal reaction conditions for BNPP hydrolysis. In all aqueous solution studies presented in this work, ZrK 2:2, which was synthesized according to a procedure described in literature,^[21] was used as a starting compound. The 2:2 nature of this POM has been previously confirmed by X-ray analysis of the solid sample^[21] and by ³¹P NMR spectroscopy of an aqueous solution at pH 4.78, which showed a single ³¹P resonance at δ = −13.49 ppm. However, in aqueous solutions Zr^{IV}-substituted POMs are prone to interconversion, and depending on the pD, temperature, reaction time, starting concentration, and ionic strength, conversion of ZrK 2:2 into ZrK 1:2^[22] can occur to result in various molar ratios of these two compounds. The stability of ZrK 2:2 in aqueous solution can be conveniently monitored by ³¹P NMR spectroscopy since both ZrK 2:2 and ZrK 1:2 are characterized by a specific ³¹P NMR spectroscopic resonance (a single resonance at δ =

–13.49 ppm for ZrK 2:2^[21] and two resonances at $\delta = -14.67$ and -14.77 ppm for ZrK 1:2^[22,23]). The two-line spectrum of ZrK 1:2 was observed owing to the presence of two units with different bonding modes with different bond lengths and bond angles, which were determined by X-ray crystallography.^[22]

The effect of pD on the solution behavior of 2.0 mM ZrK 2:2 was recently reported.^[10c] It was concluded that, whereas ZrK 1:2 was generated by increasing the pD of a solution that contained ZrK 2:2, ZrK 2:2 was typically formed by decreasing the pD of a solution that contained ZrK 1:2.^[21] A similar trend was also observed for the Zr^{IV}-substituted Wells–Dawson analogue.^[10a,24] We performed a more detailed investigation of the pD influence on speciation, which showed that when ZrK 2:2 was used as a starting compound, only the peak assigned to ZrK 2:2^[21] was observed in solution in the pD range 2.0–7.4. However, at pD 9.0 a small amount of ZrK 1:2 was formed, whereas at pD 10.4 the complete conversion of ZrK 2:2 into ZrK 1:2 and the lacunary 0:1 [α -PW₁₁O₃₉]⁷⁻ ($\delta = -10.6$ ppm)^[25] was observed.^[10c] As neutral and slightly acidic pD values favor the presence of ZrK 2:2, which is expected to be more catalytically active, a solution pD of 6.4 was selected for further studies.

To evaluate the effect of temperature on the speciation equilibria, a 2.0 mM solution of ZrK 2:2 at pD 6.4 was kept for 1 h at different temperatures that ranged from 37 to 80 °C before assessing its species distribution by ³¹P NMR spectroscopy. The spectra, shown in Figure S1 of the Supporting Information, demonstrate that temperature has no significant effect on the solution behavior of ZrK 2:2 after heating for 1 h. Only minor amounts of ZrK 1:2 were detected at temperatures above 70 °C. To further assess the influence of incubation time on the species distribution, a 2.0 mM solution (pD 6.4) of ZrK 2:2 was kept at 60 °C for a prolonged period of time, and ³¹P NMR spectra were measured after 1, 2, and 7 d. Interestingly, as Figure S2 and Table S1 in the Supporting Information show, prolonged heating time had a significant effect on the conversion, as 13.77, 22.05, and 42.88% of ZrK 1:2 were detected in solution after 1, 2, and 7 d of incubation, respectively. The effect of time on the species distribution was also determined for a 2.0 mM ZrK 2:2 solution at slightly higher pD (pD 7.8). Comparison of the ³¹P NMR spectra of solutions at pD 7.8 (Figure S3) with those for a 2.0 mM ZrK 2:2 solution at pD 6.4 (Figure S2) shows that in both cases only ZrK 2:2 was present after mixing. However, after 2 d at pD 6.4 approximately 80% of ZrK 2:2 was still present, whereas at pD 7.8, 75% of ZrK 2:2 was already converted into ZrK 1:2. Moreover, after 7 d at pD 6.4, approximately 40% of the initial amount of ZrK 2:2 was converted to ZrK 1:2, whereas at pD 7.8 a complete conversion of ZrK 2:2 into ZrK 1:2 and the monolacunary 0:1 species was observed. These experiments confirmed that higher pD values indeed favor the conversion of ZrK 2:2 into ZrK 1:2 species.

In the next step ³¹P NMR spectra of a ZrK 2:2 solution were measured in the concentration range from 1.0 to 6.0 mM after dissolution and pD adjustment to pD 6.4. Fig-

ure S4 in the Supporting Information shows that in the concentration range from 1.0 to 4.0 mM, only the ³¹P NMR spectroscopic signal of ZrK 2:2 at $\delta = -13.49$ ppm was detected, whereas at concentrations higher than 4.0 mM, minor amounts of ZrK 1:2 were observed. This trend, in which higher concentrations favor the formation of the 1:2 species, was also demonstrated for the aqueous solution behavior of Zr^{IV}-substituted Wells–Dawson POMs.^[10a] Importantly, the ³¹P spectrum of the least concentrated solution (1.0 mM) of ZrK 2:2 was also recorded by using a higher number of scans (1024 instead of 256) and did not show any evidence of ZrK 1:2 after mixing (Figure S5), thus indicating that the absence of ZrK 1:2 at concentrations lower than 4.0 mM is indeed due to the lack of conversion of ZrK 2:2 into ZrK 1:2 and not because lower concentrations prevented the detection of ZrK 1:2 by ³¹P NMR spectroscopy. Similarly to the 2.0 mM ZrK 2:2 sample, prolonged incubation times at 60 °C also resulted in increased amounts of ZrK 1:2 for 3.0 mM (Figure S6a) and 6.0 mM (Figure S6b) samples of ZrK 2:2. Figure S6a–b and Table S1 clearly show that upon heating 3.0 and 6.0 mM solutions of ZrK 2:2 at pD 6.4 for 2 d, 25.97 and 28.16% of ZrK 1:2 species were detected respectively in solution, whereas for a 1.0 mM sample, 20.42% of ZrK 1:2 was observed. Interestingly, prolonged heating for 7 d of 3.0 and 6.0 mM solutions of ZrK 2:2 also resulted in the formation of monolacunary 0:1 species (6.38% for 3.0 mM solution and 7.55% for 6.0 mM solution). The monolacunary 0:1 species was not observed in the ³¹P spectrum of ZrK 1:2 (Figure S7) recorded under the same conditions, thus suggesting that the 0:1 form originates from the decomposition of ZrK 2:2, which takes place at higher temperatures and concentrations.

As ionic strength was shown to have an influence on both the POM speciation and the rates of POM-assisted hydrolysis rates of different biomolecules,^[6c,7,8b] the dependence of the ZrK species distribution on ionic strength was also examined. ³¹P NMR spectra of 2.0 mM solutions (pD 6.4) of ZrK 2:2 in the presence of increasing concentrations (2.0 to 7.5 M) of NaClO₄ were recorded after mixing (Figure S8 in the Supporting Information). As can be seen from Figure S8 and Figure 2, higher concentrations of NaClO₄ favored the conversion of ZrK 2:2 into ZrK 1:2. This might be explained by the binding of Na⁺ ions to the POM surface and anchoring of POM units close to the Zr^{IV} center, thereby resulting in optimal binding to form and stabilize 1:2 sandwich structures.^[26] This trend was also previously observed in the case of the formation of the 1:2 lanthanide Ln/*a*₁-P₂W₁₇O₆₁ or Ln/*a*₂-P₂W₁₇O₆₁ species in the presence of Na⁺.^[26a,27]

Finally, the influence of the substrate BNPP as well as the hydrolytically inactive analogue sodium diphenyl phosphate (DPP) on the equilibria between the different Zr^{IV}-substituted Keggin-type POMs was analyzed. The concentration of ZrK 2:2 was kept constant (2.0 mM) and the concentration of BNPP was increased from 2.0 to 50.0 mM. As can be seen from Figure S9 in the Supporting Information, an increase in BNPP concentration promoted the conver-

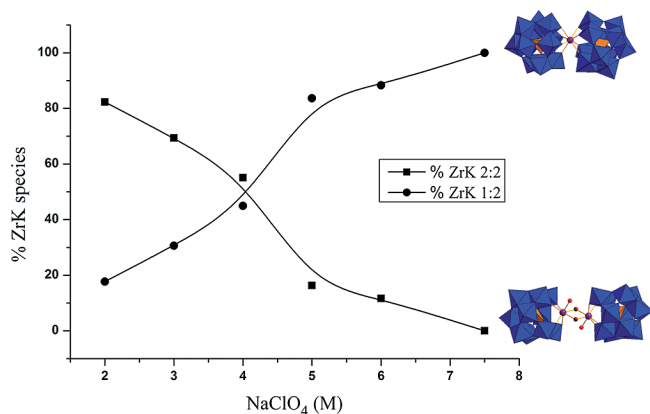


Figure 2. The percentage of ZrK 2:2 and ZrK 1:2 of a 2.0 mM solution of ZrK 2:2 in the presence of different concentrations of NaClO₄ at pD 6.4 after mixing.

sion of ZrK 2:2 into ZrK 1:2. The same trend was seen when using DPP (Figure S10). However, at identical BNPP and DPP concentrations (50.0 mM), 95.62 and 63.82% of ZrK 1:2 were detected for BNPP and DPP, respectively. Interestingly, the same concentration (50 mM) of NaClO₄ did not induce any conversion of ZrK 2:2 into ZrK 1:2. These experiments suggest that interaction of ZrK 2:2 with BNPP and DPP ligands plays an important role in Zr^{IV} POM speciation and promotes the conversion of ZrK 2:2 to ZrK 1:2.^[11a,11b]

The above results indicate that the solution chemistry of ZrK 2:2 is rather complex and is influenced by a number of different factors. Its conversion into ZrK 1:2 is favored by increasing the initial concentration of ZrK 2:2, pD, temperature, time, ionic strength, and substrate concentration. Therefore, to ensure the maximum possible amount of ZrK 2:2 in solution, an intermediate pH, lower initial concentrations as well as a low salt concentrations will be used in reactivity studies with BNPP. Unfortunately, a pure ZrK 2:2 solution will be difficult to achieve, as BNPP hydrolysis is typically observed only at elevated temperatures, typically 60–80 °C.^[6b,6e] However, as limited conversion to ZrK 1:2 was observed at 1.0 mM of ZrK 2:2 at pD 6.4 in the absence of salt, these conditions will be used in the reactivity studies to maximize the amount of ZrK 2:2 at 60 °C.

The possible interconversion between the dimeric ZrK 2:2 and monomeric ZrK 1:1 species in aqueous solution should also be taken into account. Although, to the best of our knowledge, the monomeric ZrK 1:1 has not been isolated and experimentally observed so far, the existence of dimer–monomer equilibrium has been suggested by Kholdeeva et al.^[28] for two Zr^{IV} Keggin-type POMs: $(n\text{Bu}_4\text{N})_7\text{H}[\{\text{PW}_{11}\text{O}_{39}\text{Zr}(\mu\text{-OH})_2\}]$ and $(n\text{Bu}_4\text{N})_8[\{\text{PW}_{11}\text{O}_{39}\text{Zr}(\mu\text{-OH})_2\}]$ in solution in MeCN upon addition of increasing amounts of water. In all our studies we observed only the signals assigned according to the literature to ZrK 2:2^[21] and/or ZrK 1:2.^[22,23] However if we assume that there is a condition-dependent fast exchange (with respect to the ³¹P chemical-shift timescale) between ZrK 2:2 and ZrK 1:1 in pure aqueous solution, then one averaged signal will be ob-

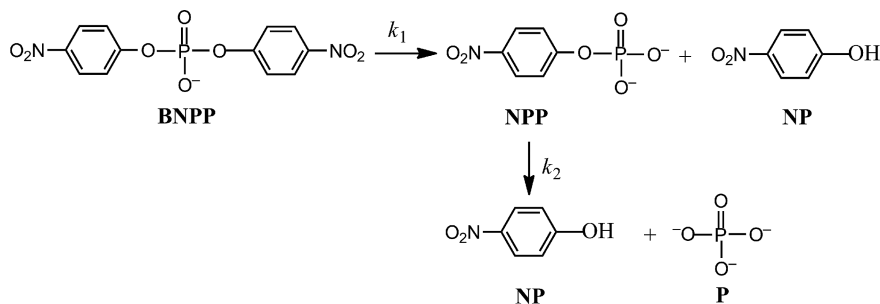
served for these two species in the ³¹P spectrum, which means that it is not possible to discriminate between them. On the basis of these arguments, the signal at $\delta = -13.49$ ppm could be also considered as a population-averaged chemical shift of ZrK 2:2 and ZrK 1:1 that exist in a fast equilibrium.

Hydrolysis of BNPP by ZrK 2:2

BNPP is typically hydrolyzed in two consecutive steps. In the first step, *p*-nitrophenol (NP) and an equimolar amount of NPP are formed. In the second step, NPP is further hydrolyzed to a second NP molecule and free phosphate (Scheme 1).^[9]

The hydrolytic reaction between BNPP and ZrK 2:2 was investigated for solutions that contained 1.0 mM of BNPP and 1.0 mM of ZrK 2:2. During the course of the reaction (pD 6.4 and 60 °C), the ¹H NMR spectra (Figure S11 in the Supporting Information) showed a gradual intensity decrease of the aromatic resonances of BNPP at $\delta = 7.33$ and 8.24 ppm and the appearance of the aromatic NP resonances at $\delta = 8.19$ and 6.96 ppm, thus indicating that hydrolysis of the P–O bond in BNPP occurred. At the end of the reaction, no BNPP resonances were detected in the ¹H and ³¹P NMR spectra (Figure S12), thus indicating a full conversion of BNPP into phosphate. Integration of the BNPP and NP ¹H NMR spectroscopic resonances at different time increments (Figure 3) allowed the calculation of the BNPP hydrolysis rate constant. A linear fitting method ($\ln[A] = k_{\text{obs}}t + \ln[A]_0$), in which A is the concentration of the substrate at time t , was used (Figure S13) and the hydrolysis rate constant for BNPP hydrolysis at pD 6.4 and 60 °C was calculated to be $(4.75 \pm 0.25) \times 10^{-6} \text{ s}^{-1}$ ($t_{1/2} = 40.5 \text{ h}$). This value represents a 320-fold rate enhancement relative to the spontaneous hydrolysis of BNPP [$k_{\text{obs}} = (1.5 \pm 0.08) \times 10^{-8} \text{ s}^{-1}$] under the same reaction conditions. A detailed comparison between the reactivity of ZrK 2:2 and that of the Wells–Dawson-type $\text{K}_{15}\text{H}[\text{Zr}(\alpha_2\text{-P}_2\text{W}_{17}\text{O}_{61})_2] \cdot 25\text{H}_2\text{O}$ POM ($6.85 \times 10^{-7} \text{ s}^{-1}$) is unfortunately not possible as its reactivity was evaluated at different reaction conditions (pD 7.2 and 50 °C);^[9] however, both POMs accelerated the rate of BNPP hydrolysis by more than two orders of magnitude over spontaneous hydrolysis.

To ensure that ZrK 2:2 was indeed required for hydrolysis, several control experiments were performed. The reaction between 1.0 mM of the Zr^{IV} salt, ZrCl₂O·8H₂O, and 1.0 mM of BNPP was examined at pD 6.4 and 60 °C. Under these conditions, the formation of insoluble Zr^{IV} hydroxy polymeric gels was observed,^[29] thus making a detailed kinetic analysis impossible. Under the same conditions, the reaction between 1.0 mM of BNPP and 1.0 mM of the monolacunary Keggin POM ($[\alpha\text{-PW}_{11}\text{O}_{39}]^{7-}$) did not show any change in rate constant relative to spontaneous BNPP hydrolysis under the same reaction conditions, thus indicating that the monolacunary Keggin POM does not promote BNPP hydrolysis and that the embedded Lewis acid Zr^{IV} ions are responsible for the observed reactivity. Lewis acid



Scheme 1. Hydrolysis of BNPP.

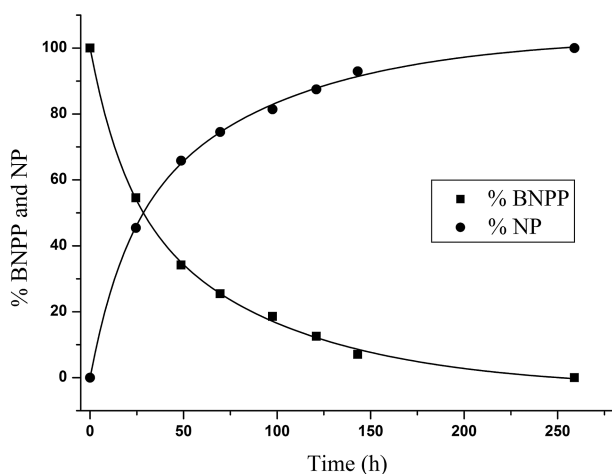


Figure 3. Percentage of BNPP and NP as a function of reaction time for the reaction between 1.0 mM of BNPP and 1.0 mM of ZrK 2:2 at pH 6.4 and 60 °C.

BNPP activation typically occurs through mono- or bidentate coordination of its phosphate oxygen atoms to Zr^{IV} . We suggest that bidentate coordination could be excluded on account of the almost coordinatively saturated nature of Zr^{IV} and the sterically hindered conformation of the bidentate POM/BNPP complex. Interestingly, under identical conditions, BNPP hydrolysis promoted by ZrK 1:2 was about five times slower [$k_{obs} = (1.14 \pm 0.01) \times 10^{-6} \text{ s}^{-1}$] than ZrK-2:2-promoted hydrolysis. ZrK 1:2 is stable even at concentrations up to 6.0 mM at pH 6.4 and 60 °C (Figure S7) and does not show any conversion into other POM species. This fivefold difference in reactivity further supports our hypothesis that, on account of the more favorable coordination environment around Zr^{IV} , ZrK 2:2 is indeed more catalytically reactive than ZrK 1:2, in which the coordination sphere around Zr^{IV} is saturated owing to coordination to two Keggin POM units.

Influence of Experimental Conditions on the Reaction Kinetics

Effect of pH on BNPP Hydrolysis

Since pH plays an important role both in the solution speciation of ZrK 2:2 as well as in phosphodiester bond hydrolysis, the effect of pH on the hydrolysis rate of BNPP

in the absence and in the presence of ZrK 2:2 was determined in the pH range 3.4 to 10.4. In this pH range, no hydrolysis of BNPP was observed after three months in the absence of ZrK 2:2. As can be seen in Figure 4, the pH dependence of k_{obs} exhibits a bell-shaped profile, with the fastest hydrolysis observed at pH 6.4. This trend further supports a Lewis acid catalyzed hydrolysis mechanism. If phosphoester bond hydrolysis were Brønsted acid mediated, an increase in k_{obs} at lower pH values would be observed.

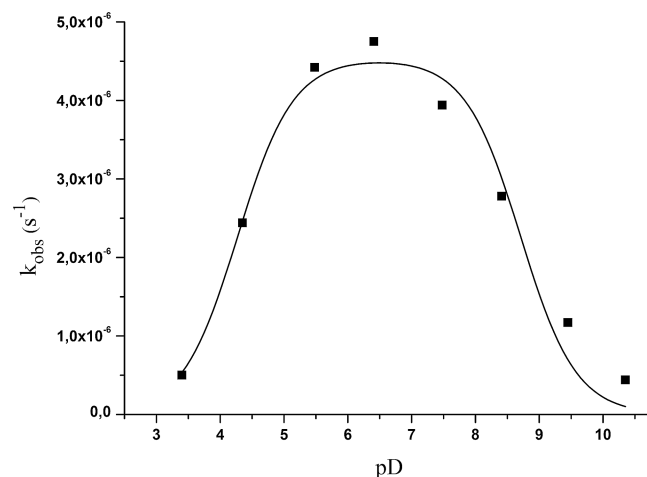


Figure 4. Dependence on pH of k_{obs} for the hydrolysis of 1.0 mM of BNPP in the presence of 1.0 mM of ZrK 2:2 at 60 °C.

The data can be fitted to a two-ionization Michaelis function (1), which describes a bell-shaped dependence of the rate constant on pH.^[30]

$$k_{obs} = k / (1 + h/K_1 + K_2/h) \quad (1)$$

In Equation (1), k_{obs} is the measured kinetic constant and k is the pH-independent turnover number. The $(1 + h/K_1 + K_2/h)$ term is known as the Michaelis pH function in which $h = 10^{-\text{pH}}$ represents the hydrogen-ion activity, whereas K_1 and K_2 are ionization constants associated with the enzyme, substrate(s), or other species in the reaction mixture.^[31] From the fitting of experimental points shown in Figure 4, the pH-independent turnover number k ($4.5 \times 10^{-6} \text{ s}^{-1}$) can be obtained. The values of $\text{p}K_1$ and $\text{p}K_2$ are 4.27 and 8.7, respectively; however, their assignment is not a straightforward task as they can originate from a broad range of intermediate species or represent a composite value.

The bell-shaped trend in the pD profile of BNPP hydrolysis by metal complexes has been previously observed^[6a,6e] and is commonly rationalized in the following way. BNPP hydrolysis in the presence of a metal complex requires OH⁻ as an active nucleophile, and as the deprotonation of water molecules is hindered at acidic pD, this results in a decrease in k_{obs} at low pD values. The increase of pD facilitates the formation of the OH⁻ nucleophiles to result in a gradual increase in k_{obs} . Upon reaching the maximum value at approximately neutral pD, a decrease in k_{obs} is usually observed owing to the formation of a hydrolytically inactive BNPP coordination complex.

However, as the speciation of ZrK 2:2 is also pD-dependent, this also has to be taken into consideration when interpreting the kinetic profile shown in Figure 4. ³¹P NMR spectroscopy has shown that during the reaction performed at pD 3.4 (Figure S14 in the Supporting Information) the intensity of the ZrK 2:2 resonance remained unchanged (as determined by integration and comparison with the resonance of the reference), thus suggesting that indeed lower reaction rates are not due to the conversion of catalytically more active ZrK 2:2 into ZrK 1:2, but rather due to the low concentration of OH⁻ nucleophiles present at low pD, as discussed above. The increase in pD facilitates deprotonation of water nucleophiles, but it also promotes conversion of ZrK 2:2 into less active ZrK 1:2, and these two opposing effects become evident at pD values greater than 6.4 when the rate of BNPP starts to decrease. The conversion of ZrK 2:2 into ZrK 1:2 was indeed evidenced in the reaction mixtures performed at pD of 6.4 and 60 °C (Figure S15). As can be seen from Figure S15, at pD 6.4 conversion of ZrK 2:2 into ZrK 1:2 was observed after 1 d, thereby resulting in a 3:1 ratio of these two POMs. As a further increase in pD showed a gradual increase in conversion of ZrK 2:2 into ZrK 1:2,^[10c] the slow hydrolysis of BNPP in alkaline solutions can be also related to the progressive conversion of ZrK 2:2 to ZrK 1:2. Moreover, in highly alkaline solutions (pD 10.4) further decomposition of ZrK 2:2 into the hydrolytically inactive monolacunary species, as demonstrated above, was observed immediately after mixing (Figure S16), thereby resulting in a complete loss of catalytic activity.

Effect of Temperature on BNPP Hydrolysis

In general, an increase in temperature results in a BNPP hydrolysis rate increase.^[6b,6e] However, as the speciation studies reported above have shown that the temperature also has significant influence on the ZrK 2:2 solution equilibria, the effect of temperature on the hydrolysis reaction rate was examined in a solution that contained equimolar amounts of BNPP and ZrK 2:2 (1.0 mM) at pD 6.4 in the temperature range from 37 to 80 °C. From the data shown in Figure S17a, the activation energy of the reaction can be calculated by using the Arrhenius equation (2).

$$\ln k_{\text{obs}} = \ln A - \frac{E_a}{R} \frac{1}{T} \quad (2)$$

In this equation, E_a represents the activation energy, R is the gas constant, and T corresponds to the temperature. Linear fitting of $\ln k_{\text{obs}}$ as a function of $1/T$ (Figure S17a in the Supporting Information) results in an experimental activation energy (E_a) of 60.16 kJ mol⁻¹, which is significantly lower than the one (121.59 kJ mol⁻¹)^[32] in the absence of ZrK 2:2 under similar reaction conditions. The Eyring equation (3) can be further used to obtain information on the activation enthalpy (ΔH^\ddagger) and entropy (ΔS^\ddagger) of the hydrolysis reaction.

$$\ln \frac{k_{\text{obs}}}{T} = \frac{-\Delta H^\ddagger}{R} \frac{1}{T} + \ln \frac{k_b}{h} + \frac{\Delta S^\ddagger}{R} \quad (3)$$

In this equation, R represents the gas constant, $k_b = 1.38 \times 10^{-23} \text{ J K}^{-1}$ is the Boltzmann constant and $h = 6.626 \times 10^{-34} \text{ J s}^{-1}$ is the Planck constant. Linear fitting of $\ln(k_{\text{obs}}/T)$ as a function of $1/T$ (Figure S17b in the Supporting Information) allows for the calculation of the enthalpy of activation, $\Delta H^\ddagger = 57.44 \text{ kJ mol}^{-1}$ and entropy of activation, $\Delta S^\ddagger = -173.16 \text{ J mol}^{-1} \text{ K}^{-1}$. The negative entropy of activation is in accordance with the expected loss of entropy as a result of the coordination of BNPP and/or NPP to the ZrK 2:2. Out of these data, the Gibbs activation energy (ΔG^\ddagger) was calculated to be 111.12 kJ mol⁻¹ at 37 °C. A similar value (96.94 kJ mol⁻¹ at 37 °C) was obtained for NPP hydrolysis by the Wells–Dawson type K₁₅H[Zr(α₂-P₂W₁₇O₆₁)₂·25H₂O] POM.^[9]

Interestingly, although speciation studies have shown that high temperatures favor conversion of ZrK 2:2 into ZrK 1:2, the rate of BNPP hydrolysis did increase as a result of an increase in temperature. As the conversion of ZrK 2:2 to ZrK 1:2 is rather slow, ZrK 2:2 is still present during the course of hydrolysis, which at higher temperatures proceeds much faster (for example, after 36 h 93.01% of BNPP is hydrolyzed at 80 °C, whereas at 37 °C only 13.24% conversion was observed). In addition, one should keep in mind that although less reactive, ZrK 1:2 also promotes hydrolysis of BNPP, and in solutions that contains both ZrK 2:2 and ZrK 1:2 species two parallel hydrolytic reactions are likely to occur.

Effect of ZrK 2:2 Concentration on BNPP Hydrolysis

In general, catalyst concentration influences the reaction rate, and to investigate the effect of ZrK 2:2 concentration on the hydrolytic reaction, rate constants were determined for a reaction mixture that contained a fixed amount of BNPP (1.0 mM) and increasing amounts of ZrK 2:2 at pD 6.4 and 60 °C (Figure 5).

The data in Figure 5 show that an increase in ZrK 2:2 concentration results in an increase in the reaction rate. The speciation solution studies have shown that higher concentrations of ZrK 2:2 result in higher amounts of catalytically less active ZrK 1:2, and this might explain the deviation from the linear trend observed in Figure 5. For example, for a 0.5 mL mixture that contained 1.0 mM of BNPP and

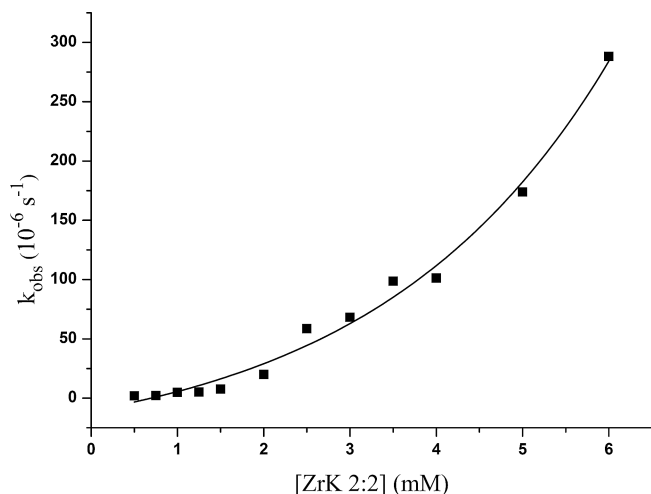


Figure 5. Influence of the concentration of ZrK 2:2 on the observed rate constant for the hydrolysis of 1.0 mM of BNPP at pD 6.4 and 60 °C.

1.0 mM of ZrK 2:2, 74.37% of ZrK 2:2, which equals to 0.37×10^{-6} mol of ZrK 2:2, was present after 1 d (Figure S15 in the Supporting Information). In contrast, a 0.5 mL mixture of 1.0 mM of BNPP and 3.0 mM of ZrK 2:2 contained 72.85% of ZrK 2:2 after one day (Figure S18), thereby resulting in 1.08×10^{-6} mol of ZrK 2:2. Similarly, when higher concentrations of ZrK 2:2 were used (6.0 mM), the conversion to ZrK 1:2 was larger (68.39% of ZrK 2:2 was present) after one day (Figure S19); however, this results in 2.05×10^{-6} mol of ZrK 2:2 present in solution. These results demonstrate that despite the fact that higher initial concentrations of ZrK 2:2 lead to more favorable conversion to ZrK 1:2, the total molar amount of ZrK 2:2 in solution is still much higher, thereby resulting in faster hydrolysis.

Interestingly, these experiments also revealed that ZrK 2:2 is able to fully hydrolyze an excess amount of BNPP, thus demonstrating one of the main principles of catalysis. Complete hydrolysis of BNPP was still observed when 1.0 mM of BNPP and 0.5 mM of ZrK 2:2 were used, which suggests that one equivalent of ZrK 2:2 is able to hydrolyze at least two equivalents of BNPP. In contrast, catalytic activity was not observed for the isopolyoxomolybdate $[\text{Mo}_7\text{O}_{24}]^{6-}$, which was converted to $[\text{P}_2\text{Mo}_7\text{O}_{23}]^{6-}$ as a result of the release of phosphate as one of the reaction products.^[6c]

Effect of Ionic Strength on BNPP Hydrolysis

The addition of salt to reactions that contain ionic species can either significantly influence or have no effect on the reaction rate. As both ZrK 2:2 and BNPP carry negative charge at pD 6.4, the influence of ionic strength on the reaction rate constant for BNPP hydrolysis was examined by adding stepwise NaClO_4 to a mixture that contained 1.0 mM of BNPP and 1.0 mM of ZrK 2:2. A large decrease in the rate constant was observed upon adding increasing

amounts of NaClO_4 (Figure 6). NaClO_4 plays a role both in the binding between BNPP and ZrK 2:2, as well as in the speciation of this POM. As control experiments with the lacunary POM showed that Zr^{IV} is essential for the catalytic activity, it is very likely that binding between ZrK 2:2 and BNPP occurs by means of coordination between the negatively charged oxygen of BNPP and the positively charged Zr^{IV} ion. Addition of salt may disrupt this interaction, resulting in lower reaction rates. However, NaClO_4 also promotes conversion of ZrK 2:2 into ZrK 1:2 (Figures S20–S22 in the Supporting Information). As can be seen from Figure S20, at pD 6.4, 22.06% of ZrK 1:2 is detected in a reaction mixture that contained 0.05 M NaClO_4 , whereas in the presence of 0.5 M NaClO_4 (Figure S21) 73.35% of ZrK 1:2 was observed. Upon increasing the concentration of NaClO_4 to 5.0 M (Figure S22), a full conversion of ZrK 2:2 into ZrK 1:2 was observed immediately after mixing.

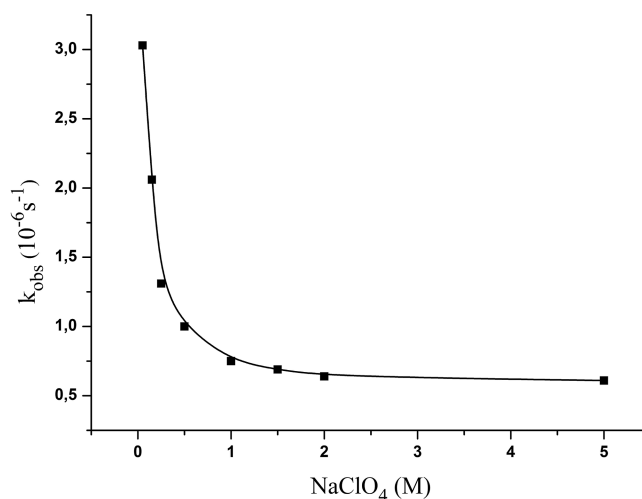


Figure 6. Influence of the concentration of NaClO_4 on the hydrolysis rate constant for the reaction of 1.0 mM of BNPP and 1.0 mM of ZrK 2:2 at pD 6.4 and 60 °C.

Inhibition Study

To gain further insight in the interaction between BNPP and ZrK 2:2, the inhibitory effect of the nonreactive BNPP analogue, diphenyl phosphate (DPP), which lacks activating nitro groups, was examined. In the control experiments no hydrolysis was observed for a 1.0 mM DPP solution both in the absence and in the presence of 1.0 mM of ZrK 2:2 after four months. The hydrolysis of 1.0 mM of BNPP was followed in the presence of 1.0 mM of ZrK 2:2 and increasing amounts (1.0 to 100 mM) of DPP (Figure 7). As can be seen from Figure 7, the rate constant of BNPP hydrolysis significantly decreased upon adding increased amounts of DPP. Again DPP plays a dual role, both affecting the interaction between BNPP and ZrK 2:2 as well as the solution speciation of ZrK 2:2. In both cases DPP has a negative effect, as on the one hand it competes with BNPP for the binding to Zr^{IV} and on the other hand it largely shifts equilibrium toward the formation of ZrK 1:2, as discussed above.

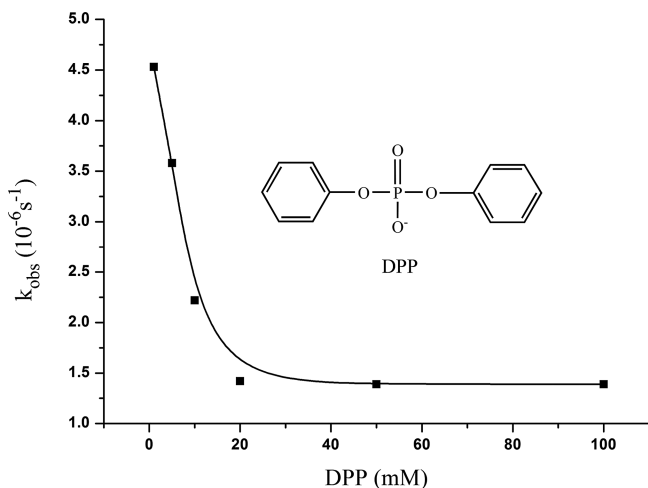


Figure 7. Influence of the concentration of DPP on the observed rate constants for the hydrolysis of 1.0 mM of BNPP in the presence of 1.0 mM of ZrK 2:2 at pD 6.4 and 60 °C.

Conclusion

A detailed ^{31}P NMR spectroscopic aqueous solution study on the Zr^{IV} -substituted POM $(\text{Et}_2\text{NH}_2)_8\{\alpha\text{-PW}_{11}\text{O}_{39}\text{Zr}(\mu\text{-OH})(\text{H}_2\text{O})\}_2\cdot 7\text{H}_2\text{O}$ (ZrK 2:2) that describes the influence of pD, temperature, reaction time, ionic strength, and ZrK 2:2 or substrate concentration allowed for a full characterization of the speciation equilibria that exist under different experimental conditions. This study is of importance as during the last decade it was shown that metal-substituted POMs can be used as promoting agents or catalysts for a broad range of reactions. As a result, speciation studies are necessary to identify the most reactive species in solution as well as to optimize the reaction conditions. The results obtained in this study showed that ZrK 2:2 converts into ZrK 1:2, which is expected to be catalytically less active, upon increase of pD, ZrK 2:2 concentration, and ionic strength. The conversion became more pronounced at higher temperatures and after prolonged reaction times. Kinetic experiments indeed demonstrated that ZrK 2:2 is the more hydrolytically active species for the hydrolysis of the phosphoester bonds in the DNA model substrate bis(4-nitrophenyl) phosphate (BNPP). Moreover, there was a clear link between the observed influence of pD, ZrK 2:2 concentration, temperature, and ionic strength on the BNPP hydrolysis rate and the aqueous solution behavior of ZrK 2:2, thus demonstrating the usefulness of such detailed speciation studies. The present study demonstrates the potential of Zr^{IV} -substituted POMs as artificial phosphatases and contributes to the further development of POMs as Lewis acid catalysts for the hydrolysis of biomolecules. Future studies will be focused on the hydrolytic activity of this POM towards adenosine triphosphate (ATP), the RNA model substrate HPNP, and DNA/RNA fragments.

Experimental Section

Materials: The Zr^{IV} -substituted Keggin POM, $(\text{Et}_2\text{NH}_2)_{10}\text{-}[\text{Zr}(\text{PW}_{11}\text{O}_{39})_2]\cdot 7\text{H}_2\text{O}$ ^[22] (ZrK 1:2), and binuclear Zr^{IV} -substituted Keggin POM, $(\text{Et}_2\text{NH}_2)_8\{\alpha\text{-PW}_{11}\text{O}_{39}\text{Zr}(\mu\text{-OH})(\text{H}_2\text{O})\}_2\cdot 7\text{H}_2\text{O}$ ^[10c,21] (ZrK 2:2), were prepared as described in the literature. Disodium 4-nitrophenyl phosphate (NPP; $\text{C}_6\text{H}_4\text{NO}_6\text{PNa}_2\cdot 6\text{H}_2\text{O}$), sodium bis(4-nitrophenyl) phosphate (BNPP; $\text{C}_{12}\text{H}_8\text{N}_2\text{NaO}_8\text{P}$), sodium diphenyl phosphate (DPP; $\text{C}_{12}\text{H}_{10}\text{NaO}_4\text{P}$), DCl, and NaOD were purchased from Acros and used without any further purification.

Kinetic Measurements: Solutions that contained 1.0 mM of BNPP and 1.0 mM of ZrK 2:2 were prepared in D_2O . The final pD of solution was adjusted with minor amounts of 10% DCl and 15% NaOD solutions in D_2O . The pH-meter value was corrected by using the equation: $\text{pD} = \text{pH meter reading} + 0.41$.^[33] The pD of the samples was measured in the beginning and at the end of hydrolysis, and the difference was typically less than 0.5 to 1 pD units owing to the release of free phosphate as one of the products of the reaction. The reaction mixture was kept at constant temperature, and ^1H NMR spectra were measured at certain time intervals during the hydrolytic reaction to calculate the observed rate constant (k_{obs}) by the integral method.

NMR Spectroscopy: ^1H and ^{31}P NMR spectra were recorded with a Bruker Avance 400. ^1H spectra were referenced with respect to 0.5 mM of 2,2,3,3-[D_4]-3-(trimethylsilyl)propionic acid (TMSP) as an internal standard, whereas 25% phosphoric acid was used as an external reference for ^{31}P spectra.

Supporting Information (see footnote on the first page of this article): NMR spectra and hydrolysis data.

Acknowledgments

T. N. P.-V. and P. S. (BOF fellowship) thank the KU Leuven for financial support. T. K. N. L. thanks the Vietnamese Government and KU Leuven for a doctoral fellowship. G. A. thanks Fonds voor Wetenschappelijk Onderzoek (FWO) Flanders for a postdoctoral fellowship. The authors acknowledge the CMST COST Action (CM1203, Polyoxometalate Chemistry for Molecular Nanoscience) for financial support in terms of STSM applications.

- a) A. Proust, R. Thouvenot, P. Gouzerh, *Chem. Commun.* **2008**, 1837–1852; b) D.-L. Long, R. Tsunashima, L. Cronin, *Angew. Chem. Int. Ed.* **2010**, *49*, 1736–1758; *Angew. Chem.* **2010**, *122*, 1780; c) D.-L. Long, R. Tsunashima, L. Cronin, *Angew. Chem.* **2010**, *122*, 1780–1803.
- a) M. Carraro, S. Gross, *Materials* **2014**, *7*, 3956–3989; b) A. Proust, B. Matt, R. Villanneau, G. Guillemot, P. Gouzerh, G. Izzet, *Chem. Soc. Rev.* **2012**, *41*, 7605–7622.
- a) J. M. Clemente-Juan, E. Coronado, A. Gaita-Arino, *Chem. Soc. Rev.* **2012**, *41*, 7464–7478; b) K. M. Seemann, A. Bauer, J. Kindervater, M. Meyer, C. Besson, M. Luysberg, P. Durkin, W. Pyckhout-Hintzen, N. Budisa, R. Georgii, C. M. Schneider, P. Kogerler, *Nanoscale* **2013**, *5*, 2511–2519.
- a) J. J. Stracke, R. G. Finke, *J. Am. Chem. Soc.* **2011**, *133*, 14872–14875; b) N. V. Izarova, M. T. Pope, U. Kortz, *Angew. Chem. Int. Ed.* **2012**, *51*, 9492–9510; c) A. Sartorel, M. Bonchio, S. Campagna, F. Scandola, *Chem. Soc. Rev.* **2013**, *42*, 2262–2280.
- a) A. Ogata, S. Mitsui, H. Yanagie, H. Kasano, T. Hisa, T. Yamase, M. Eriguchi, *Biomed. Pharmacother.* **2005**, *59*, 240–244; b) T. Yamase, *J. Mater. Chem.* **2005**, *15*, 4773–4782; c) B. Hasenknopf, K. Micoine, E. Lacote, S. Thorimbert, M. Malacria, R. Thouvenot, *Eur. J. Inorg. Chem.* **2008**, 5001–5013; d)

- X. H. Wang, F. Li, S. X. Liu, M. T. Pope, *J. Inorg. Biochem.* **2005**, *99*, 452–457; e) M. Cindric, T. K. Novak, S. Kraljevic, M. Kralj, B. Kamenar, *Inorg. Chim. Acta* **2006**, *359*, 1673–1680; f) S. Mitsui, A. Ogata, H. Yanagie, H. Kasano, T. Hisa, T. Yamase, M. Eriguchi, *Biomed. Pharmacother.* **2006**, *60*, 353–358; g) H. Stephan, M. Kubeil, F. Emmerling, C. E. Müller, *Eur. J. Inorg. Chem.* **2013**, 1585–1594.
- [6] a) G. Absillis, E. Cartuyvels, R. Van Deun, T. N. Parac-Vogt, *J. Am. Chem. Soc.* **2008**, *130*, 17400–17408; b) N. Steens, A. M. Ramadan, G. Absillis, T. N. Parac-Vogt, *Dalton Trans.* **2010**, *39*, 585–592; c) G. Absillis, R. Van Deun, T. N. Parac-Vogt, *Inorg. Chem.* **2011**, *50*, 11552–11560; d) L. Van Lokeren, E. Cartuyvels, G. Absillis, R. Willem, T. N. Parac-Vogt, *Chem. Commun.* **2008**, 2774–2776; e) E. Cartuyvels, G. Absillis, T. N. Parac-Vogt, *Chem. Commun.* **2008**, 85–87.
- [7] P. H. Ho, E. Breynaert, C. E. A. Kirschhock, T. N. Parac-Vogt, *Dalton Trans.* **2011**, *40*, 295–300.
- [8] a) H. Phuong Hien, K. Stroobants, T. N. Parac-Vogt, *Inorg. Chem.* **2011**, *50*, 12025–12033; b) P. H. Ho, T. Mihaylov, K. Pierloot, T. N. Parac-Vogt, *Inorg. Chem.* **2012**, *51*, 8848–8859.
- [9] S. Vanhaecht, G. Absillis, T. N. Parac-Vogt, *Dalton Trans.* **2012**, *41*, 10028–10034.
- [10] a) G. Absillis, T. N. Parac-Vogt, *Inorg. Chem.* **2012**, *51*, 9902–9910; b) K. Stroobants, E. Moelants, H. G. T. Ly, P. Proost, K. Bartik, T. N. Parac-Vogt, *Chem. Eur. J.* **2013**, *19*, 2848–2858; c) H. G. T. Ly, G. Absillis, T. N. Parac-Vogt, *Dalton Trans.* **2013**, *42*, 10929–10938; d) H. G. T. Ly, G. Absillis, S. R. Bajpe, J. A. Martens, T. N. Parac-Vogt, *Eur. J. Inorg. Chem.* **2013**, 4601–4611.
- [11] a) C. Boglio, B. Hasenknopf, G. Lenoble, P. Rémy, P. Gouzerh, S. Thorimbert, E. Lacôte, M. Malacria, R. Thouvenot, *Chem. Eur. J.* **2008**, *14*, 1532–1540; b) N. Dupré, P. Rémy, K. Micoine, C. Boglio, S. Thorimbert, E. Lacôte, B. Hasenknopf, M. Malacria, *Chem. Eur. J.* **2010**, *16*, 7256–7264; c) M. Carraro, N. Nsouli, H. Oelrich, A. Sartorel, A. Sorarù, S. S. Mal, G. Scorrano, L. Walder, U. Kortz, M. Bonchio, *Chem. Eur. J.* **2011**, *17*, 8371–8378; d) S. S. Mal, N. H. Nsouli, M. Carraro, A. Sartorel, G. Scorrano, H. Oelrich, L. Walder, M. Bonchio, U. Kortz, *Eur. J. Inorg. Chem.* **2009**, *49*, 7–9; e) M. Sadakane, M. H. Dickman, M. T. Pope, *Eur. J. Inorg. Chem.* **2001**, *40*, 2715–2719; f) L. Coyle, P. S. Middleton, C. J. Murphy, W. Clegg, R. W. Harrington, R. J. Errington, *Dalton Trans.* **2012**, *41*, 971–981; g) S. Zhao, L. Huang, Y.-F. Song, *Eur. J. Inorg. Chem.* **2013**, 1659–1663; h) K. Nomiyama, K. Ohta, Y. Sakai, T. Hosoya, A. Ohtake, A. Takakura, S. Matsunaga, *Bull. Chem. Soc. Jpn.* **2013**, *86*, 800.
- [12] P. M. Cullis, E. Snip, *J. Am. Chem. Soc.* **1999**, *121*, 6125–6130.
- [13] a) E. L. Hegg, J. N. Burstyn, *Coord. Chem. Rev.* **1998**, *173*, 133–165; b) M. Komiyama, N. Takeda, H. Shigekawa, *Chem. Commun.* **1999**, 1443–1451; c) R. Kramer, *Coord. Chem. Rev.* **1999**, *182*, 243–261; d) A. Blasko, T. C. Bruice, *Acc. Chem. Res.* **1999**, *32*, 475–484.
- [14] a) A. Radzicka, R. Wolfenden, *Science* **1995**, *267*, 90–93; b) J. E. Thompson, T. G. Kutateladze, M. C. Schuster, F. D. Venegas, J. M. Messmore, R. T. Raines, *Bioorg. Chem.* **1995**, *23*, 471–481.
- [15] J. Rawlings, W. W. Cleland, A. C. Hengge, *J. Am. Chem. Soc.* **2006**, *128*, 17120–17125.
- [16] a) D. E. Wilcox, *Chem. Rev.* **1996**, *96*, 2435–2458; b) N. Sträter, W. N. Lipscomb, T. Klabunde, B. Krebs, *Angew. Chem. Int. Ed. Engl.* **1996**, *35*, 2024–2055; *Angew. Chem.* **1996**, *108*, 2158.
- [17] a) F. Mancin, P. Scrimin, P. Tecilla, *Chem. Commun.* **2012**, *48*, 5545–5559; b) D. Desbouis, I. P. Troitsky, M. J. Belousoff, L. Spiccia, B. Graham, *Coord. Chem. Rev.* **2012**, *256*, 897–937.
- [18] J. Chin, M. Banaszczyk, *J. Am. Chem. Soc.* **1989**, *111*, 4103–4105.
- [19] A. Calderón, A. K. Yatsimirsky, *Inorg. Chim. Acta* **2004**, *357*, 3483–3492.
- [20] a) K. Stroobants, V. Goovaerts, G. Absillis, G. Bruylants, E. Moelants, P. Proost, T. N. Parac-Vogt, *Chem. Eur. J.* **2014**, *20*, 9567–9577; b) K. Stroobants, G. Absillis, E. Moelants, P. Proost, T. N. Parac-Vogt, *Chem. Eur. J.* **2014**, *20*, 3894–3897.
- [21] K. Nomiyama, Y. Saku, S. Yamada, W. Takahashi, H. Sekiya, A. Shinohara, M. Ishimaru, Y. Sakai, *Dalton Trans.* **2009**, 5504–5511.
- [22] C. N. Kato, A. Shinohara, K. Hayashi, K. Nomiyama, *Eur. J. Inorg. Chem.* **2006**, *45*, 8108–8119.
- [23] L. Cai, Y. Li, C. Yu, H. Ji, Y. Liu, S. Liu, *Inorg. Chim. Acta* **2009**, *362*, 2895–2899.
- [24] Y. Saku, Y. Sakai, K. Nomiyama, *Inorg. Chim. Acta* **2010**, *363*, 967–974.
- [25] a) G. M. Maksimov, R. I. Maksimovskaya, *Polyhedron* **1996**, *15*, 4275–4276; b) M. N. Sokolov, E. V. Chubarova, E. V. Peresypkina, A. V. Virovets, V. P. S. Fedin, *Russ. Chem. Bull.* **2007**, *56*.
- [26] a) C. Zhang, R. C. Howell, Q.-H. Luo, H. L. Fieselmann, L. J. Todaro, L. C. Francesconi, *Eur. J. Inorg. Chem.* **2005**, *44*, 3569–3578; b) C. Zhang, R. C. Howell, K. B. Scotland, F. G. Perez, L. Todaro, L. C. Francesconi, *Eur. J. Inorg. Chem.* **2004**, *43*, 7691–7701.
- [27] C. Zhang, L. Bensaid, D. McGregor, X. F. Fang, R. C. Howell, B. Burton-Pye, Q. H. Luo, L. Todaro, L. C. Francesconi, *J. Cluster Sci.* **2006**, *17*, 389–425.
- [28] O. A. Kholdeeva, G. M. Maksimov, R. I. Maksimovskaya, M. P. Vanina, T. A. Trubitsina, D. Y. Naumov, B. A. Kolesov, N. S. Antonova, J. J. Carbó, J. M. Poblet, *Eur. J. Inorg. Chem.* **2006**, *45*, 7224–7234.
- [29] a) A. Singhal, L. M. Toth, J. S. Lin, K. Affholter, *J. Am. Chem. Soc.* **1996**, *118*, 11529–11534; b) R. A. Moss, J. Zhang, K. G. Ragnathan, *Tetrahedron Lett.* **1998**, *39*, 1529–1532.
- [30] A. Cornish-Bowden, L. Endrenyi, *Biochem. J.* **1986**, *234*, 21–20.
- [31] V. Lykourinou, A. I. Hanafy, K. S. Bisht, A. Angerhofer, L.-J. Ming, *Eur. J. Inorg. Chem.* **2009**, 1199–1207.
- [32] a) J. Chin, M. Banaszczyk, V. Jubian, X. Zou, *J. Am. Chem. Soc.* **1989**, *111*, 186–190; b) P. S. Low, J. L. Bada, G. N. Somero, *Proc. Natl. Acad. Sci. USA* **1973**, *70*, 430–432.
- [33] P. K. Glasoe, F. A. Long, *J. Phys. Chem.* **1960**, *64*, 188–190.

Received: July 31, 2014

Published Online: September 29, 2014